Dynamic mechanical behavior of syntactic iron foams with glass microspheres

Dynamic mechanical behavior of syntactic iron foams with glass microspheres

Lorenzo Peroni [a], Martina Scapin [a,*], Massimiliano Avalle [a], Jörg Weise [b], Dirk Lehmhus[c]

[a] *Politecnico di Torino, Department of Mechanical and Aerospace Engineering, Corso Duca degli Abruzzi, 24 – 10129 Torino, Italy*
[b] *Fraunhofer Institute for Manufacturing Technology and Advanced Materials, Wiener Straße 12, 28359 Bremen, Germany*
[c] *ISIS Sensorial Materials Scientific Centre, University of Bremen, Wiener Straße 12, 28359 Bremen, Germany*

In this work, the mechanical behavior of syntactic foams made of hollow glass microspheres mixed in an iron matrix was investigated. This type of material is interesting since, when compared to other types of metal foams, it offers greatly increased quasi-static compressive strength, though at lower maximum porosity and thus higher density. Moreover it maintains the advantages and useful properties of metal foams such as thermal and environmental resistance.

In particular, the strain-rate sensitivity response was studied. The experimental characterization was performed by means of compression tests at three strain-rate levels: at the highest strain-rate level a SHPB was used. Type and content of glass microspheres were also studied.

The experimental results showed that the compression behavior of syntactic foams, similarly to the other types of foams, is strongly affected by all the examined factors. For what concerns the strain-rate, it was found to increase material characteristics in almost all cases. The influence of the matrix behavior on the composite was identified as the determining parameter in this respect.

In order to evaluate the results obtained with the described tests campaign, the experimental data were further elaborated by means of an empirical analytical strain-rate sensitive model. The dependency of the material response on model parameters was widely discussed.

1. Introduction

In recent years, the attention of several researchers was focused on the development and characterization of a particular class of foam structures, the syntactic foam, in which hollow spheres are dispersed in a continuum matrix.

From a mechanical point of view, the behavior of syntactic foams is quite similar to the behavior of a metal matrix composite combined with features of conventional foams. As a matter of fact, there are two distinct phases: a matrix in which there is a dispersion of particles, hollow in particular. In general, the resulting behavior of a composite material depends on both matrix and dispersed second phase mechanical properties but also on their interaction. In the preparation of the syntactic foam, different types of particles can be used, e.g. foam glass granules, metal spheres, ceramic spheres [1,2] and glass bubbles [3–7]. The matrix can be polymeric [3–7] or metallic [1,2,8–10].

When compared to correspondent dense materials, this class of materials exhibits lower density combined with high strength and energy-absorbing capabilities. This combination makes this class of materials suitable for several applications, like structural sandwich cores, impact-absorbing applications, crash safety and packaging. The mechanical response is influenced by several parameters, such as density, type, structure and dimensions of the particles, type of matrix and loading conditions [11,12]. When contrasted to metal foams based on the powder compact melting or the APM process [13], the iron matrix syntactic foams combine lower maximum porosity and higher density with greatly increased quasi-static compressive strength while showing the typical deformation characteristics of foams. As a matter of fact, the achievable level of porosity stays below the respective value of other types of foams. Thus, the lowest density which can be obtained is higher, or similarly, from the point of view of porosity, the maximum porosity is lower with respect to other foams.

In several works the influence of the reinforcement content on the material behavior was investigated. Tao and Zhao [2] analyzed the quasi-static compressive behavior of an aluminum matrix syntactic foam varying the volume percentage of the matrix content. This was reached by toughening the matrix with aluminum particles improving the ductility and the compressive strength of the foam. The quasi-static behavior in compression was studied also by Swetha and Kumar [3] depending on the filler properties. Viot et al.[7] showed that varying the microsphere volume fraction (and con-sequently the density) produce the effect of changing the damage mechanism. In particular, for low particle content the main dam-age mechanism is the fracture of the microspheres. On the other

* Corresponding author. Tel.: +39 0161226479; fax: +39 0161226322.
E-mail address: martina.scapin@polito.it (M. Scapin).

hand, for high particle content the material damage is due to the matrix failure. The latter aspect can be explained by the fact that, due to the high particles content, the amount of bonds in the matrix is limited. Similar studies were performed by Gupta et al. [6] and Shunmugasamy et al. [5], in which the behavior of the syntactic foam was investigated for different strain-rates, polymeric matri-ces, micro-balloon types, and percentages of glass content. Dou et al. [9] analyzed the cenospheres-pure aluminum syntactic foam focusing the attention on the influence of the particle dimension in different strain-rate loading conditions, comparing the results with the pure matrix samples. In [9], the authors also provided the calculation of the strain-rate sensitivity parameter and devel-oped a three parameters data-fitting analytical model to predict the dynamic compressive strength of the foam. In [14] different aspects, such as morphology, topology, sphere wall thickness and strain-rate sensitivity were analyzed. The objective was the investigation of the macroscopic behavior of metallic hollow sphere structures by means of computational simulations.

In this work the attention was focused on the mechanical characterization of the behavior of a metallic syntactic foam in a wide range of strain-rates. Since a metallic syntactic foam shows properties both of metallic foam and metal matrix composite, its behavior at high strain-rate is shown to be quite complex. The quasi-static mechanical behavior of different types of syntactic foams under uniaxial compressive loading condition was widely investigated in recent years, see e.g. [2,3,6]. Several studies were also performed in order to understand the syntactic foam behavior at high strain-rates, see e.g. [1,4,5,7,9]. In general, it was found that the compressive strength of the syntactic foam is controlled to a large degree by the strength of the matrix. This implies also that the strain-rate sensitivity of the foam is close to the matrix one.

The syntactic foam analyzed by the authors was made of a pure iron matrix with a dispersion of hollow glass microspheres. It was obtained by means of metal powder injection molding (MIM) [15]. The parameters taken into account in the evaluation of the material behavior were the microsphere content (5, 10 and 13% in weight), the type of microspheres (S60HS and iM30K) and the strain-rate. The experimental tests performed were compression tests from quasi-static up to high dynamic loading conditions, covering 6 orders of magnitude in strain-rate. The choice of this type of loading (i.e. compressive), even though apparently too simplistic, still covers most of the envisaged energy absorption applications.

Starting from the analysis of the experimental results, the authors propose the numerical fit of the data with an empirical strain-rate sensitive model [16]. The authors widely discussed the influence of each parameter of the model, focusing the attention on their trends in function of both type and percentage of glass.

2. Iron syntactic foams

Several production methods for syntactic foams exist, such as melt stirring, melt infiltration or powder metallurgy processes [17]. In the current literature, production techniques based on the infil-tration of solid structures or loose bulks of the hollow elements by metal melts represent the dominant approach. Since metal melts do not usually wet the hollow particles, pressure-assisted infiltra-tion techniques like gas-pressure infiltration or squeeze-casting are frequently used [18]. For alloys with high melting temperatures, like iron or steel, liquid infiltration of microsphere structures is extremely difficult. Only few techniques like gas-pressure infiltra-tion are available and the combined impact of high pressure and temperature during the filling stage can lead to the destruction of the micro bubbles which have wall-thicknesses of few microns.

Alternative approaches to the melt infiltration can be based on powder metallurgical techniques like pressing or metal powder injection molding (MIM [15]). In the latter process, which is closely related to polymer injection molding, the forming step is carried out at moderate temperature (110–140 °C), whereas the subsequent pressureless sintering process is done at temperatures of around 2/3 to 4/5 of the melting point of the respective material. Obviously, this still exceeds the softening point of a lot of microsphere types. However, it could be shown that the interaction of metal powder and microspheres leads largely to a preservation of the shape and a limited reduction in the size of the hollow spheres – even though they have only weak internal residual strength at the applied sinter-ing temperatures. The feasibility of this approach could be shown for several high-melting alloys like pure Fe, FeCu3 or FeNi36.

3. Experimental procedure for material production

Following the above-mentioned approach, syntactic Fe99.7 foams containing different weight percentages of glass microspheres were synthesized: for sample production, a feedstock was prepared which contained approximately 50 vol.% of pure Fe (Dr. Fritsch GmbH, purity 99.7, $d_{50} = 1.4\,\mu m$), a binding agent as well as different glass microspheres weight fractions (5, 10 and 13 wt%) and two different glass microsphere types (S60HS e iM30K). The hollow elements are commercial hollow glass microspheres, produced by 3M and made of soda-lime borosilicate glass. Both of them are specially formulated for a high strength-to-weight ratio. This guarantees greater survivability during injection molding. The main properties of these glass microspheres are reported and compared in Table 1. The two types of glass microspheres have the same density (0.6 kg/dm^3). Since the average diameter of the microspheres is higher in the case of the S60HS glass, their estimated wall thickness exceeds that of the iM30K variant. Nevertheless, the maximum allowable injection pressure to obtain a percentage of failed microspheres between 80% and 90% is higher for the latter.

The values given for the weight percentage of glass microspheres refer to the combined mass of metal and glass in the final composite material (sintered part). In addition to these components, the metal injection molding feedstock contained a polymer–wax binder which was matched in volume to the Fe content. Mixing and feedstock homogenization took place using a Brabender-CE equipment. The final feedstock was injected into a tensile test specimen mould at 110 °C (mould temperature 50 °C) and 4 bar using a HEK injection molding machine. The binder was removed via a combined chemical (48 h at 25 °C in hexane) and thermal process (holding at 500 °C for 60 min after heating-up at 0.1 K/min) with subsequent sintering for 90 min at 900 °C in H_2 atmosphere following a temperature ramp-up at 5 K/min. For reference samples (pure Fe samples), the same feedstock was used without the addition of microspheres.

Different mixtures were prepared and the properties of the sintered materials are shown in Table 2. Using 0.6 kg/dm^3 as density of the glass microspheres and 7.87 kg/dm^3 for that of pure iron, the theoretical density of perfect syntactic foams was calculated. The composition affects the resulting material density that varies from the pure iron density to less than half of its value at 13 wt% microspheres content. In Fig. 1, the results of the light microscopy of the metallographic sections of the syntactic foams analyzed in this work are shown. It can be seen that the foam quality is very good for Fe with S60HS glass bubbles, whereas in the case of iM30K more destroyed glass bubbles were found. This might be explained by increased chemical interactions at the larger interface between matrix and the glass bubbles of the iM30K type.

The samples were provided in dog-bone shaped specimen (Fig. 2a). The rounded shape, with approximately 4mm diam-eter, is particularly fit for manufacturing purposes. Preliminary tests performed in tension showed that the introduction of glass

Table 1
Main properties of the two types of glass microspheres used.

Product designation (S series)	Material	Average diameter (μm)	Estimated wall thickness (μm)	Maximum injection pressure (MPa)
iM30K	Soda-lime borosilicate glass	18	0.804	124
S60HS	Soda-lime borosilicate glass	30	1.341	200

Table 2
Mixtures for the production of the analyzed syntactic foams.

	Fe 99.7	S60HS			iM30K		
wt% glass	0	5	10	13	5	10	13
Theoretical density (kg/dm^3)	7.87	5.26	4.05	3.58	5.26	4.05	3.58
Measured density (kg/dm^3)	7.34	5.08	4.07	3.34	5.21	4.26	3.82
Ratio = measured density/theoretical density	0.93	0.97	1.01	0.93	0.99	1.05	1.07

microspheres causes an important loss of strength and ductility. In this loading condition, plastic deformation is not possible, and de-cohesion of the two phases is at the origin of brittle failure and strong decrease in the ultimate tensile strength. These considerations, and the fact that the behavior under tensile load is less relevant for most applications of this class of materials, motivated the authors to perform the strain-rate sensitivity analysis in compression only.

The compression tests were performed on simple cylindrical specimens (nominally 4, 6 and 8 mm in length, 4 mm of diameter, see Fig. 2b) cut from the central part of the tensile specimens. Each sample (a total of about 70 samples were obtained) was measured and weighted to obtain dimensional and density information. Average measured density values were obtained for each class of samples as reported in Table 2. Fig. 3 shows the relation between glass weight percentage and resultant foam density obtained from measurements of the compression samples. The data were reported for both two types of glass and each set of data was interpolated with a third order polynomial function constraining the Fe density for the 0 wt% of glass. As expected, the foam density behavior for the two types of glass becomes more similar by reducing the glass percentage.

By calculating the ratio between the theoretical density value and the measured value (Table 2) for the pure iron samples, a residual porosity of about 7% was found. For what concerns the syntactic foam, a ratio greater than unity could be due to the shrinkage of the hollow spheres during the sintering process or their failure during the injection process. The latter, however, was not supported by metallographic studies.

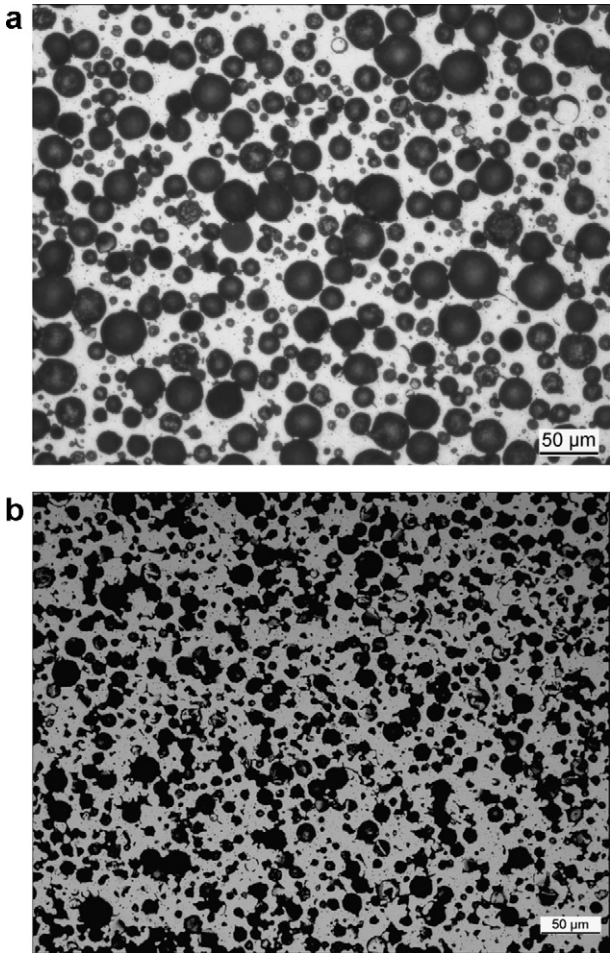

Fig. 1. Light microscopy of the metallographic sections of syntactic foams with different types of hollow spheres (10 wt%): (a) S60HS and (b) iM30K.

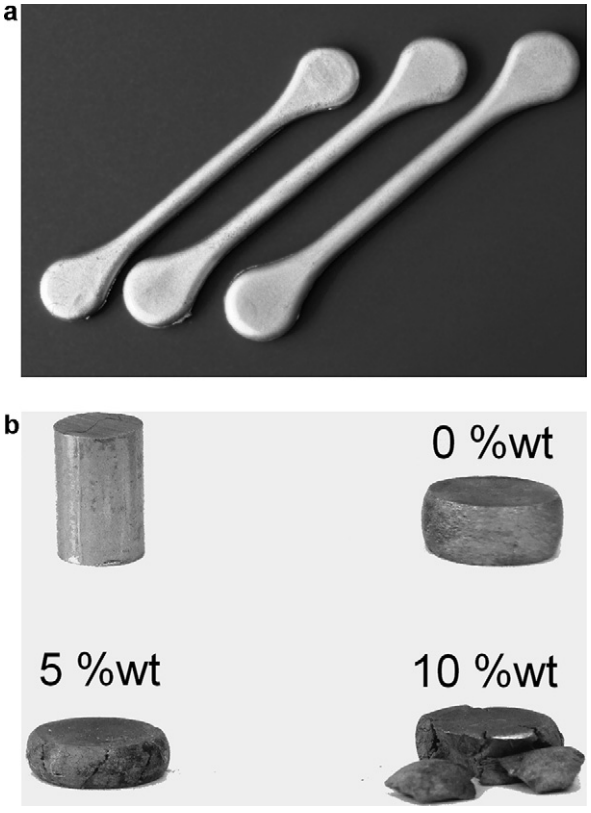

Fig. 2. Tensile specimens of syntactic foam (a), from the left: 0 wt%, 5 wt%, 10 wt%; cylindrical compression specimens before and after the test (b).

4. Experimental procedure for material testing

Like most conventional foams, syntactic foams show a lower tensile strength and ductility in comparison to the compact alloys. For syntactic foams, however, the mechanical behavior is much more complex due to the above-mentioned hybrid nature (metal matrix composite/foam).

In this work the strain-rate influence on the mechanical response was investigated by compression tests covering six orders of magnitude in strain-rate on samples with different glass microsphere percentages and types. For each parameters combination, at least three valid tests were performed.

The experimental tests were performed starting from quasi-static loading conditions up to high dynamic ones. All the experimental tests were performed in the Reliability and Safety Laboratory of the Politecnico di Torino (Vercelli Technological Pole).

The low-speed tests (at about $10^{-2}\,s^{-1}$ of strain-rate) were performed with a general purpose electro-mechanical material testing machine, Zwick Z100. This equipment is able to apply loads up to 100 kN, measured by a 100 kN load cell, at a speed of up to 5 mm/s.

Medium speed tests, at about 80 mm/s loading rate (that corresponds to strain-rate between $10\,s^{-1}$ and $20\,s^{-1}$, depending on the initial specimen length) were performed with a DARTEC HA100 universal servo-hydraulic material testing machine. In this case the load was measured with a 30 kN piezoelectric load cell, while the displacement was measured with a 100 mm LVDT.

Dynamic tests were performed by means of a standard Split Hopkinson Pressure Bar (SHPB) setup (Fig. 4a). The apparatus was actuated by a pneumatic gas-gun (1.5 m long) and was composed of two bars made in high strength steel of 10 mm diameter and 3 m length. The striker bar used in these tests was 1 m long: with this setup the impact velocity is about 8 m/s. This implies that with the adopted specimen diameter (which determines the ratio between transmitted and incident waves) and lengths (which determine the strain-rate once the reflected wave has been measured), the actual strain-rates were between 1000 s^{-1} and 2000 s^{-1}. Measurements of strain in the bars were performed with HBM resistance strain-gages conditioned with a 3 MHz bandwidth amplifier. Acquisition was made with a 2.5 MHz NI acquisition board managed by a LabView program.

In Fig. 4b an example of the wave profiles obtained during a SHPB test is depicted. The curves reported in the diagram are the incident and the reflected waves (labeled *input*) measured by the strain-gauge station on the input bar and the transmitted one (labeled *output*) measured on the output bar. As can be deduced from the ratio between the wave amplitude, the deformability of this type of foam is such that the test can be performed using classical metallic bars, without using specific methodologies suitable for softer materials [19].

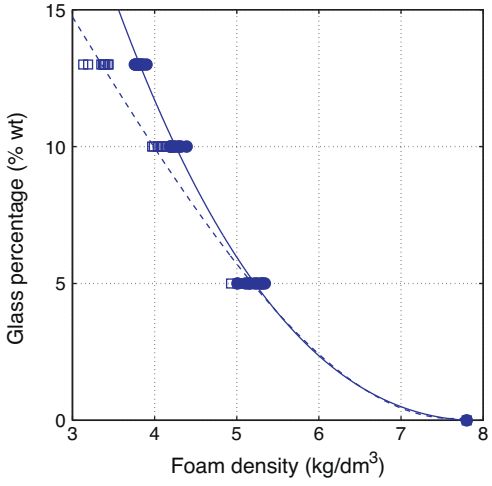

Fig. 3. Relation between glass weight percentage and resultant foam density obtained from measurements of the compression samples, for the two types of glass (S60HS: □; iM30K: ●): data interpolations with a third order polynomial function (S60HS: dashed line; iM30K: solid line).

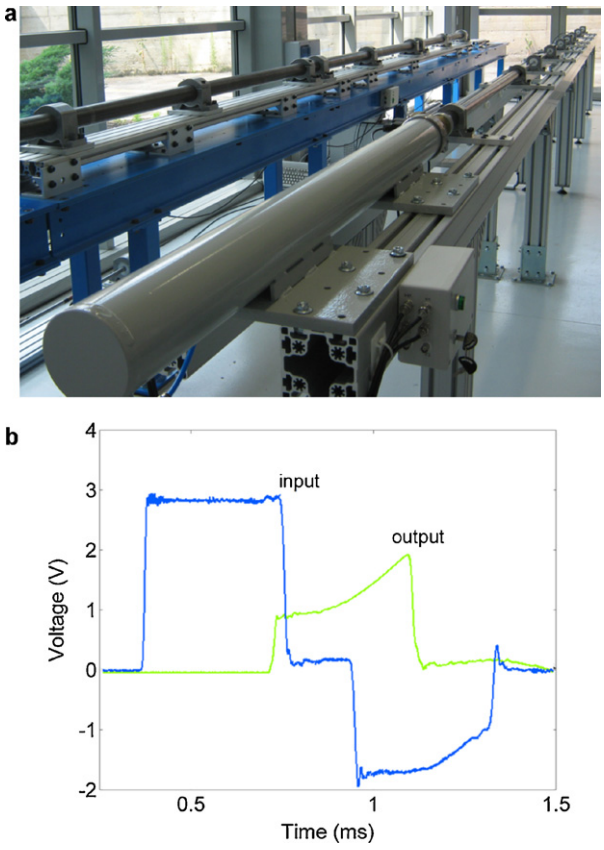

Fig. 4. SHPB setup used for high dynamic tests of the syntactic foam samples (a); example of the measured waves profile during a SHPB test in terms of voltage vs. time (b). Reliability and Safety Laboratory of the Politecnico di Torino (Vercelli Technological Pole).

Experimental results are reported in the following figures. Figs. 5 and 6 report the stress–strain characteristics of the two glass microsphere types respectively, varying the weight content and the loading rate. As for all foamed materials, in compression, after first yield, there is a plateau phase followed by densification. Of course, for unfilled material the plateau is non-existent, whereas for only 10% weight content an almost horizontal plateau is observed, ranging from 5% to 30–40% of strain. As it becomes clear from Figs. 5 and 6, the strength drop is pronounced as soon as a small per-centage of glass microspheres is added, but it is much reduced when passing on from the 5% to 10% weight content, especially regard-ing yield. This is probably due to the fact that the contribution of the glass microspheres balances the strength loss caused by the reduction of iron content. This observation is important because it justifies the considerable interest in this class of materials, since greater weight saving can be achieved while maintaining good energy absorption capability, thus increasing the overall efficiency.

In general and as expected, in case of glass microspheres with a higher strength (iM30K), the higher the percentage of glass, the more the material behaves like a true foam, showing a more pronounced stress plateau. Under high strain-rate loading conditions, however, the fragile nature of the glass leads to premature failures and less capacity of energy absorption.

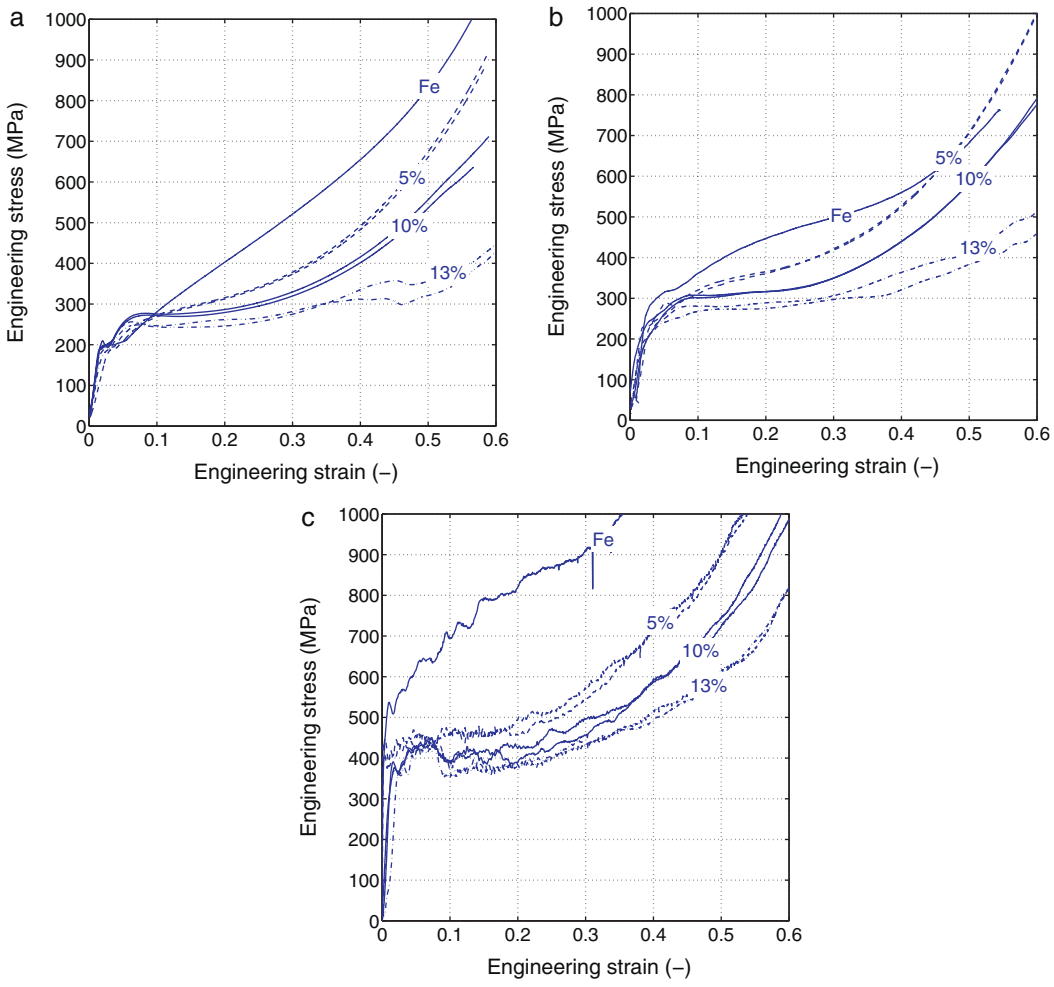

Fig. 5. Stress–strain characteristics for the iM30K syntactic foams: (a) quasi-static tests ($10^{-2}\,s^{-1}$); (b) medium strain-rate tests ($10–20\,s^{-1}$); (c) high-speed SHPB tests ($1000–2000\,s^{-1}$). For all test cases only two samples are reported for sake of clarity but repeatability was always very good.

In contrast, in case of glass with a lower strength (S60HS), the contribution of the glass microspheres to the strength of the foam is much more important. Most of the foam resistance is governed by the glass, which induces a more brittle and weaker behavior. For weight content higher than 10 wt% the plateau extends more than 50% of deformation, even with a decrease of strength with strain. This is observed at all the strain-rates, and, as for the other glass, it is even more critical under high dynamic load. The effect of the type of microspheres is depicted in Figs. 7 and 8, in which the quasi-static and dynamic stress–strain curves obtained for the two glasses (*H* identifies the iM30K glass and *L* identifies the S60HS glass) are compared at different particles weight contents. Compar-ison of quasi-static and SHPB tests underlines the typical strain-rate sensitivity of the reference material, pure iron, which leads to an increase in upper yield strength from 202 MPa to 512 MPa (see Figs. 5 and 6). In terms of plateau onset stress, microsphere rein-forced materials show less increase. From Fig. 7c, the embrittlement caused by S60HS glass for high weight content previously dis-cussed in comparison with the iM30K-based foam, is evident both in static and dynamic regime. Looking at quasi-static loading con-ditions, a smooth progression over the strain range is observed for most of the sample types. No drop in stress level, proper of macroscopic fracture, is seen below 50% of strain in each sample containing either 5 or 10 wt% of microspheres. However, 13 wt%S60HS samples show such fracture events at approximately 5–15%of strain, whereas they are located at higher strains of about 35–45%in 13 wt% iM30K samples. Generally, smoothness of stress–strain curves reflects ductility in foams. Thus it can be concluded that the smaller scale iM30K microspheres coincide with a more ductile behavior showing some strain hardening. In contrast, the almost zero slope of the plateau region seen in S60HS based samples is associated with some amount of brittle fracture, but also with higher levels of energy absorption efficiency.

5. Discussion: analysis of the results

In order to evaluate the results obtained with the described tests campaign, the experimental data were further analyzed by means of an empirical analytical model [16,21], which expresses the flow stress as follows:

$$\sigma(\varepsilon,\dot{\varepsilon}) = A_0(1-e^{-m\varepsilon})\left(1+A_1\ln\frac{\dot{\varepsilon}}{\dot{\varepsilon}_0}\right)+B_0\frac{\varepsilon^n}{(1-\varepsilon)^p}\left(1+B_1\ln\frac{\dot{\varepsilon}}{\dot{\varepsilon}_0}\right)$$
$$= A(1-e^{-m\varepsilon})+B\frac{\varepsilon^n}{(1-\varepsilon)^p} \quad (1)$$

where σ, ε and $\dot{\varepsilon}$ are the stress, strain and strain-rate, respectively, and A (or A_1 and A_0), m, B (or B_1 and B_0), n and p are the model parameters. Viscous effects are taken into account by means of a widespread engineering approach multiplying the stress–strain characteristic by a strain-rate factor in the same form of that proposed in [20] and implemented in most simulation codes (LS-DYNA, Abaqus, etc.). This approximation, although being a rough

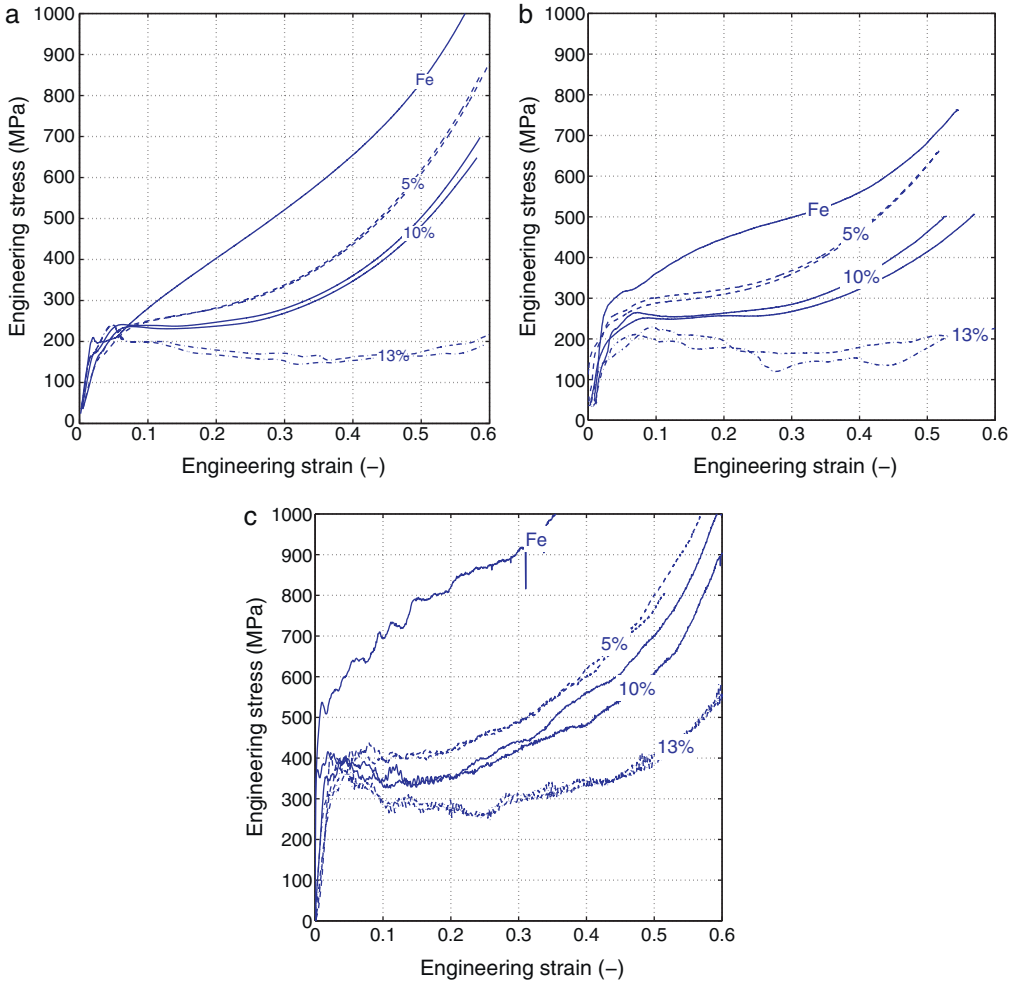

Fig. 6. Stress–strain characteristics for the S60HS syntactic foams: (a) quasi-static tests ($10^{-2}\,s^{-1}$); (b) medium strain-rate tests ($10–20\,s^{-1}$); (c) high-speed SHPB tests ($1000–2000\,s^{-1}$). For all test cases only two samples are reported for sake of clarity but repeatability was always very good.

interpretation of the physical behavior, gives satisfactory results in most applications.

The first term of the model describes the small strain behav-ior, whereas the second term comes in to model the densification region. It is, therefore, a two components mechanical model. Some distinctive features of the first term are fundamental for the desired characteristics of the model. The tangent modulus in the origin (ε = 0) is equal to the parameter mA, which can be considered the initial elastic modulus of the foam. The first term of the model also has a horizontal asymptote for high strain values near to A. It means that above a certain strain value, the stress, defined by this term, is nearly constant and equals the parameter A, which can be considered the plateau stress of the foam. Finally, the use of the exponential function gives a relevant improvement in the fit of the curve knee at the connection of the elastic region with the plateau region, as a consequence of the appropriate choice of the exponent m. As described in [16], the yield strength of the foam is proportional to the value of A, which can be considered a valid indi-cator for the strength of the material. This can be derived imposing the yield as the intersection point between the stress–strain curve from the model and a straight line passing through the origin and with slope equal to a certain percentage (R) of the estimated elas-tic modulus (mA). It is possible to demonstrate that the stress at the intersection depends on the value of R, but it is independent from the value of m: the yield stress is a given fraction of A for any value chosen for the percentage R. Due to small dimensions, non-planarity of the opposite faces and non-uniformity of the material of the specimens, the first part of the mechanical response could be affected by major uncertainties. Since the value of m does not influence the yield stress, this procedure for the yield identification is not influenced by any errors in the elastic modulus estimation. On the other hand, if a procedure based on the offset (e.g. $Rp_{0.2}$) was used, the estimation would be less reliable and accurate, as most affected by the slope of the first part of the stress–strain curve.

The second part of the model allows the description of the densification behavior, imposing a vertical asymptote for the strain condition $\varepsilon = 1$.

The parameters identification procedure described below is based on the mean squared error minimization method for a single objective optimization process. This corresponds to perform a simple 1D numerical analysis of the compression behavior of the material, using the optimization tool of MATLAB. The optimization problem is defined as follows:

$$\min_{C} \left\| \boldsymbol{\sigma}_{ex} - \boldsymbol{\sigma}_{th}(C) \right\|_2 \tag{2}$$

in which C identifies the set of the model parameters chosen as optimization variables, $\boldsymbol{\sigma}_{ex}$ is the stress vector obtained experimentally, $\boldsymbol{\sigma}_{th}(C)$ is the theoretical stress vector obtained by evaluating the function of Eq. (1) in each strain experimental point.

Each experimental stress–strain curve in the quasi-static regime was fit with the model of Eq. (1) and a set of 5 parameters (A, m, B, p, n) was found for each curve at the end of the optimization

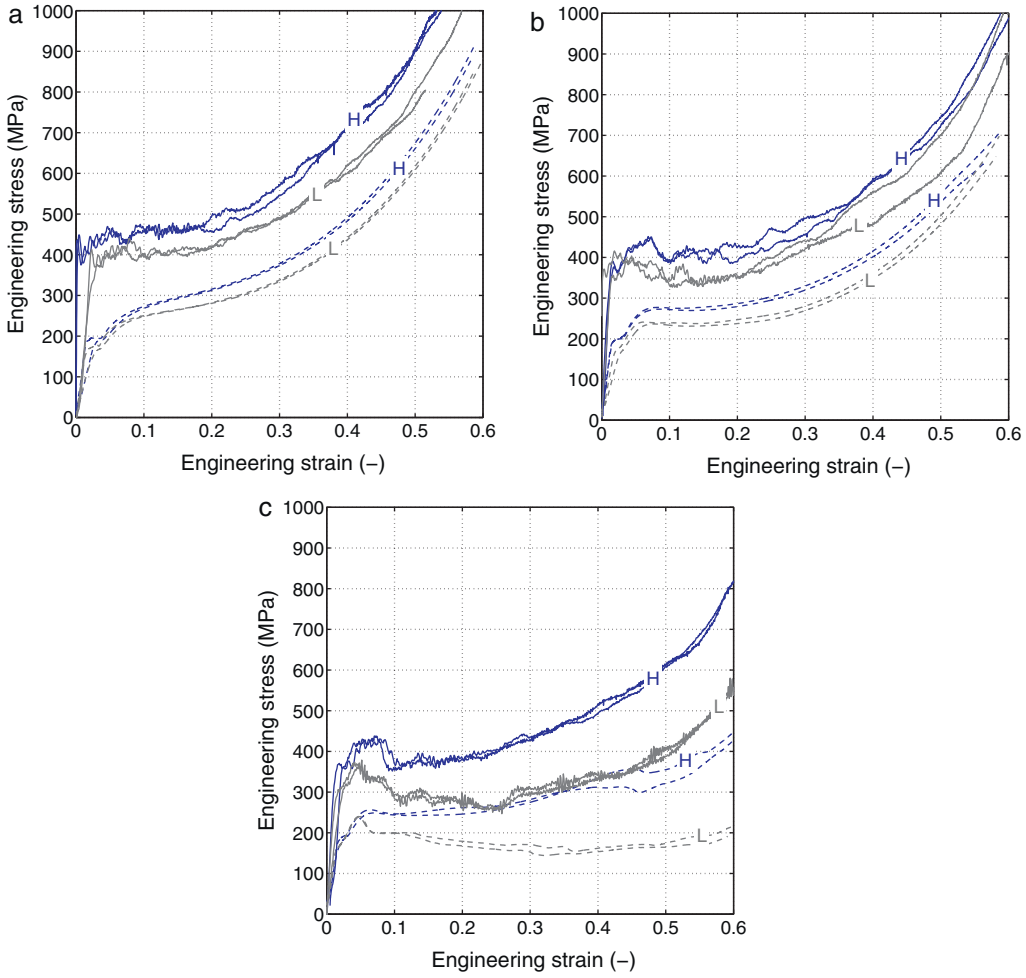

Fig. 7. Comparison of the engineering stress–strain characteristics for the S60HS (L) and iM30K (H) syntactic foams at quasi-static (lower set of curves, dashed lines) and high dynamic loading conditions (higher set of curves, solid line): (a) 5% glass weight content; (b) 10% glass weight content; (c) 13% glass weight content.

process. The experimental results of the syntactic foam at 13 wt% of S60HS glass show a marked decreasing behavior. This could be due to the fact that this type of foam with a great amount of glass decreases its strength losing the capability to increase the stress approaching the densification. The analytical model used in this work is not able to predict this behavior. For this reason, the second part of the model was not considered (B, n, $p = 0$) in case of 13 wt% S60HS syntactic foam. On the other hand the second part of the model was considered for all the considered density in case of the iM30K-based foam.

For the data fit in the medium and high strain-rate regimes, the parameters n and p were fixed. They were estimated for each type and for each weight percentage of glass as the aver-age value obtained from the quasi-static results (Table 3). This can be justified by the fact that the maximum strain level reached in the tests is too far from the limit condition ε = 1. More-over, the final strain is different from curve to curve. These aspects should produce a great variability of the optimized val-ues if three parameters on the second part of the model are used. The parameters chosen as optimization variables for the dynamic tests are A, m and B for both iM30K at 5, 10 and 13 wt%and S60HS at 5 and 10 wt%, while A and m for 13 wt% S60HS foam. At the end of the second optimization step a set of these parameters was obtained for each dynamic experimental curve. The results obtained for each parameter are discussed below. In Table 3 the final (global) set of parameters for the two foams are reported.

In Fig. 9 two examples of data interpolation with this model are presented, for iM30K glass samples in static and dynamic loading conditions. As it appears clear from Fig. 9, the model is able to reconstruct very well the trend of the experimental data both in static and dynamic regime, if each curve is reproduced with its own set of optimized parameters.

Figs. 10 and 11 summarize the results regarding the A model parameter, which explained before, is strictly related to the plateau stress of the foam i.e. to its energy absorption. In particular, Fig. 10a shows the dependence of the A parameter from the microspheres content and Fig. 10b the dependence of the A parameter from den-sity. The results depicted in Fig. 10a were interpolated by a linear function in order to describe the A vs. wt% behavior of the two types of glass at two different strain-rate levels (quasi-static and high strain-rate). It is important to underline that for the two glasses, a common point was forced for wt% = 0. This constraint is justi-fied since the behavior of the two materials becomes much similar reducing the glass content and has to be the same when all the glass is removed (pure Fe specimen). The density of the foam is a quan-tity much more interesting from an engineering point of view with respect to wt%: in Fig. 10b, the same results of Fig. 10a are reported and transformed accordingly to the relation of Fig. 3.

Fig. 11 shows the dependence of the A parameter from strain-rate. In particular, Fig. 11a shows the results obtained in case of S60HS and Fig. 11b in case of iM30K. In both cases, the experimental results are concentrated at three different strain-rates: 10^{-2}, 10 and 10^{3} s^{-1}. The experimental data (grouped by weight percentage)

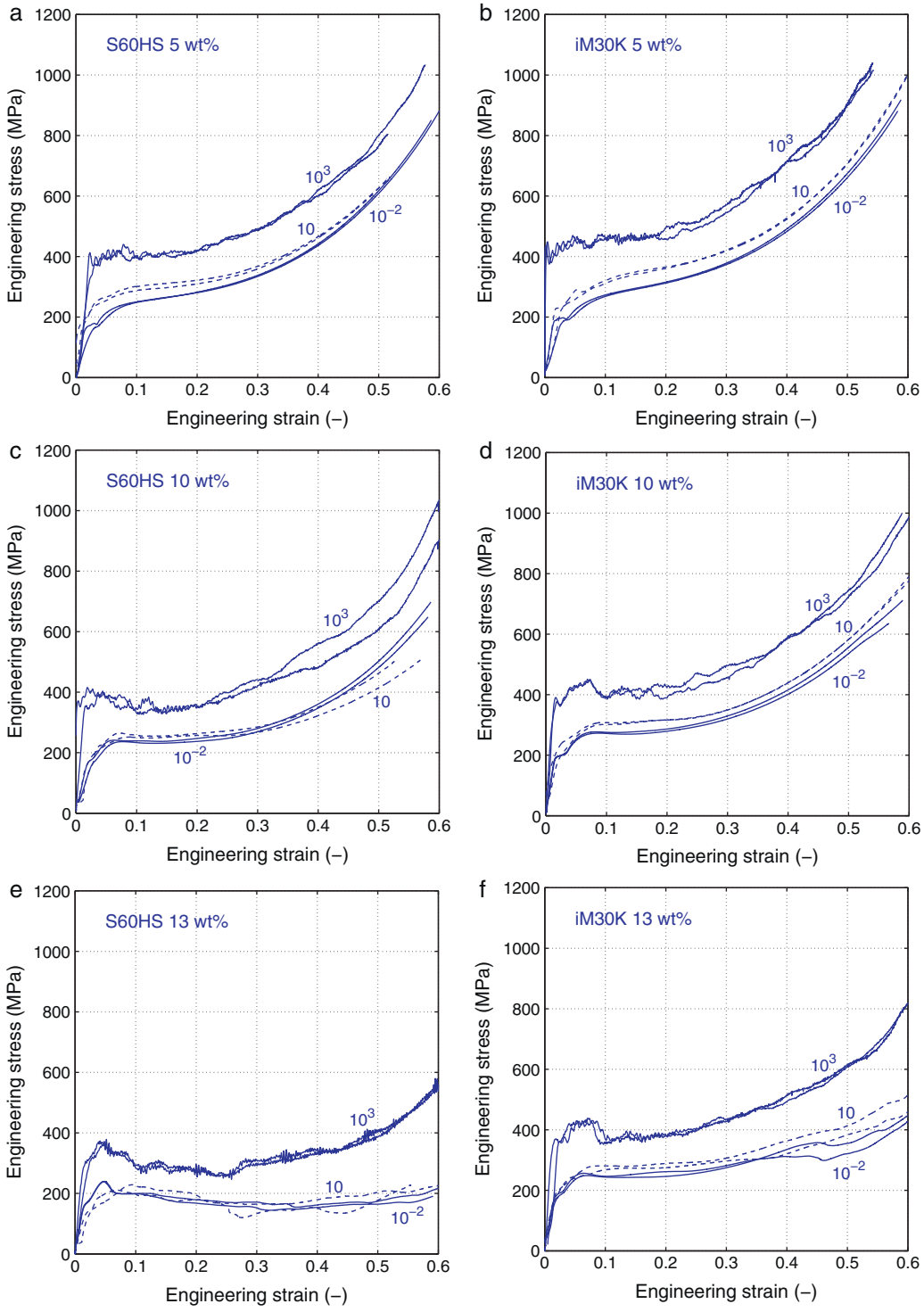

Fig. 8. Comparison of the stress–strain characteristics for the S60HS (a, c and e) and iM30K (b, d and f) syntactic foams varying the strain-rate: (a and b) 5% glass weight content; (c and d) 10% glass weight content; (e and f) 13% glass weight content.

were fitted, with respect to the first part of the model (Eq. (1)), in which

$$A = A_0 \left(1 + A_1 \ln \frac{\dot{\varepsilon}}{\dot{\varepsilon}_0}\right) \tag{3}$$

In this sense, a piecewise linear interpolation with respect to the strain-rate in logarithmic scale was performed. In more details, the bilinear behavior (as in the Johnson-Cook model implemented in LS-DYNA [22]) is represented by a stress threshold (which corresponds to the value of the parameter A of static tests, equal to A_0) for loading rates less than $\dot{\varepsilon}_0$. This means that until $\dot{\varepsilon}_0$ the strain-rate effects are negligible. On the other hand, for strain-rate greater than $\dot{\varepsilon}_0$, the Johnson-Cook relation presents a certain slope. In this work the first part (horizontal line) of the piecewise interpolation was obtained from the quasi-static data. The second part (sloping line) was governed by the tests at 10 and $10^3\,s^{-1}$. Consequently, the value of $\dot{\varepsilon}_0$ is determined by the intersection of the two lines.

For all the considered test series (2 types of glass and 3 different weight contents), the $\dot{\varepsilon}_0$ is comprised between 1 and $10\,s^{-1}$ and the A_0A_1 parameter (that is the slope of the Johnson-Cook line)

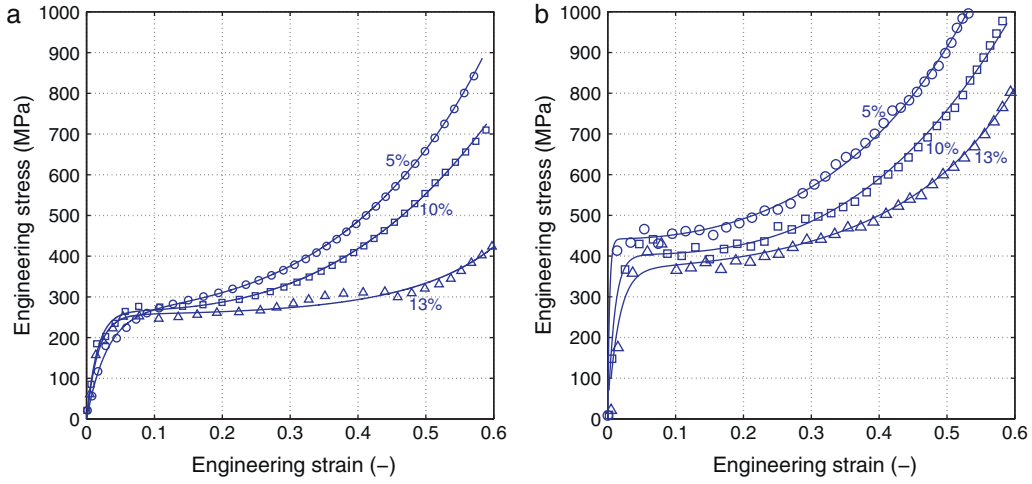

Fig. 9. Empirical model fits (lines) of experimental data (markers): tests on iM30K samples (a) static, (b) dynamic.

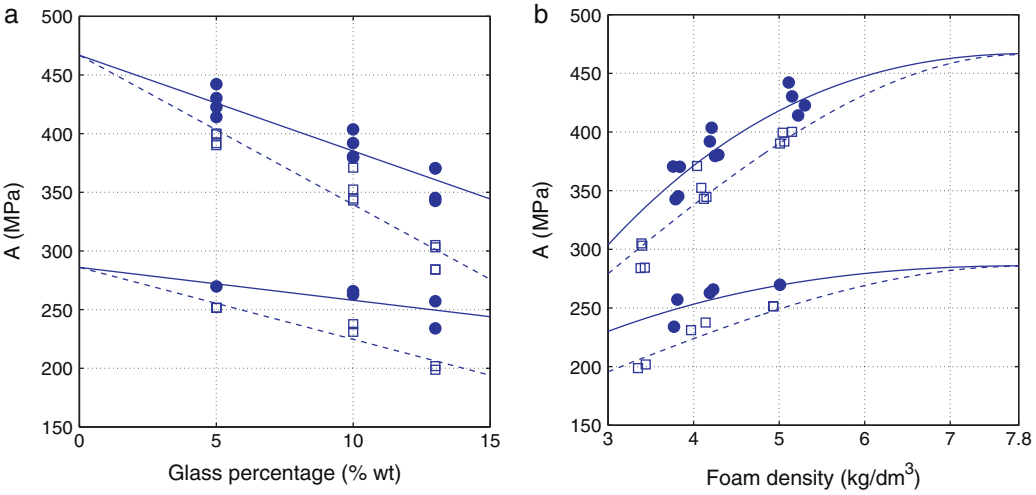

Fig. 10. Overview of model interpolation results for quasi-static (lower set of data) and dynamic (higher set of data): (a) variation of the parameter *A* in function of glass wt%; (b) variation of the parameter *A* in function of density. In the diagrams: (●) represents the results of the compressive tests and the solid lines the model fit performed on iM30K-based samples; (□) represents the results of the compressive tests and the dashed lines the model fit performed on S60HS-based samples.

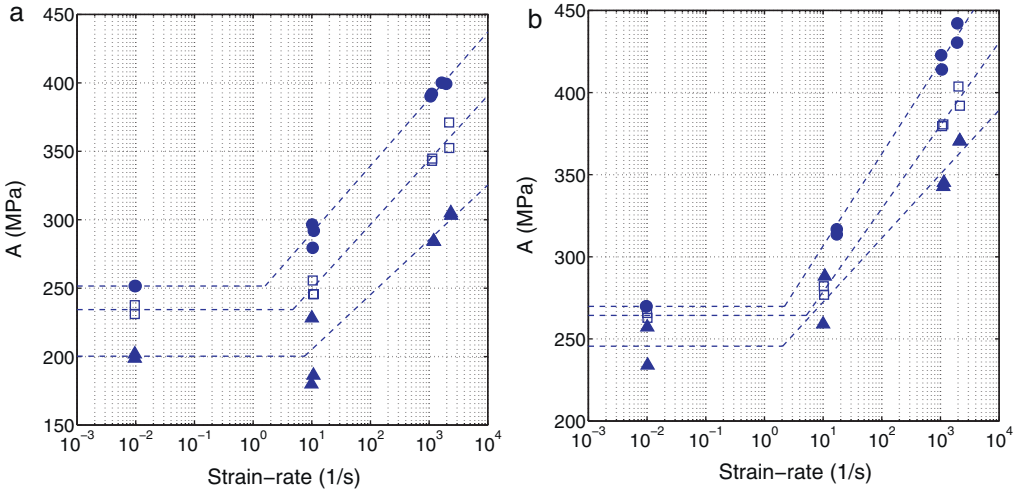

Fig. 11. Overview of model interpolation results: variation of the parameter *A* in function of strain-rate for S60HS (a) and iM30K (b). In the diagrams: (●) represents the results of the compressive tests performed on the 5 wt% foams; (□) represents the results of the compressive tests performed on the 10 wt% foams; (▲) represents the results of the compressive tests performed on the 13 wt% foams; dashed lines are the bilinear interpolations with a Johnson-Cook like strain-rate sensitive material model.

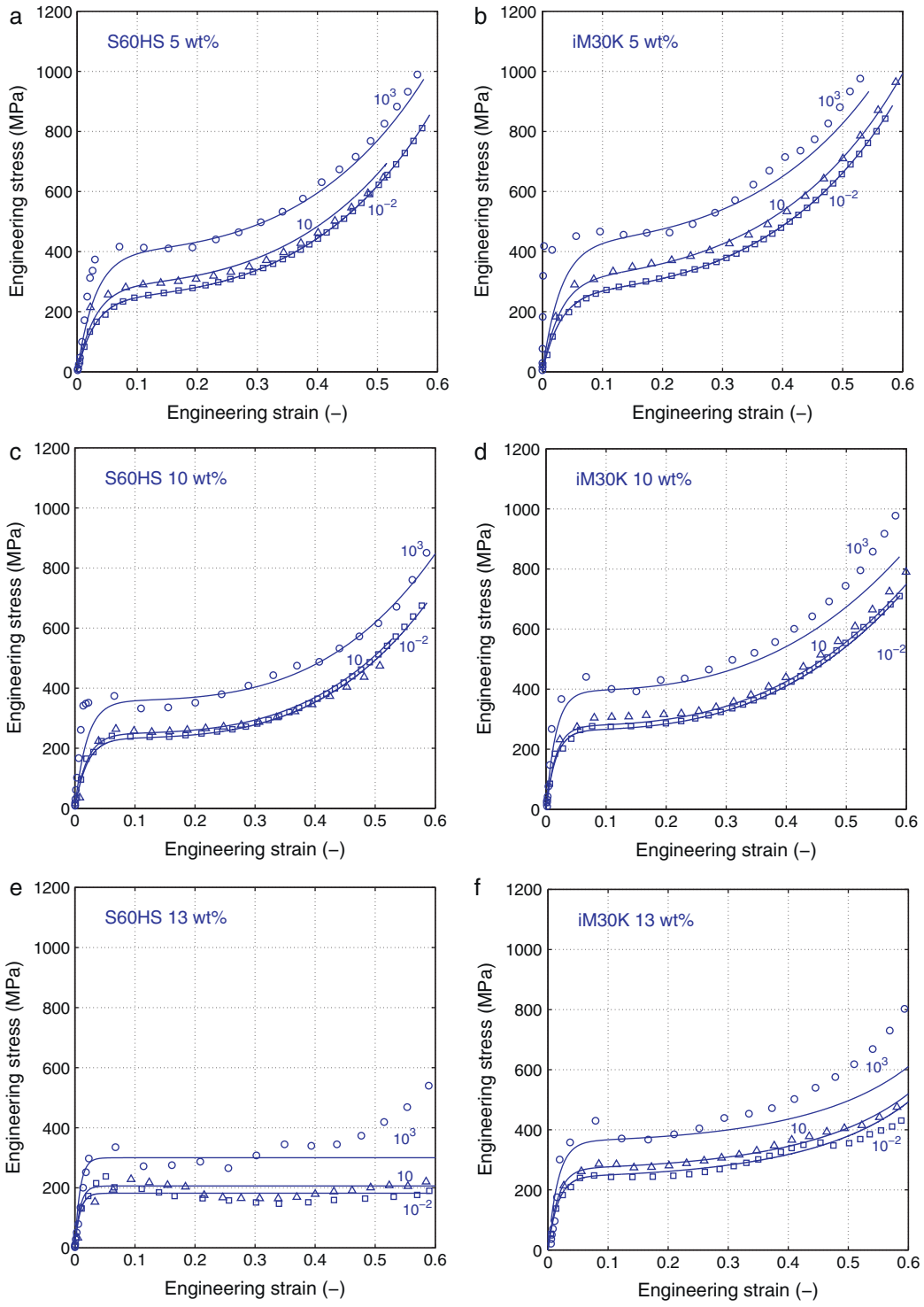

Fig. 12. Comparison between experimental data (markers) and model prediction (line) in terms of engineering stress–strain curves for the S60HS (a, c and e) and iM30K (b, d and f) syntactic foams varying the strain-rate: (a and b) 5% glass weight content; (c and d) 10% glass weight content; (e and f) 13% glass weight content.

varies little from one series to another (Table 3). However, for all the considered foams, the strain-rate sensitive of the A parameter is significant and comparable with a pure BCC metal, like iron [20]. This allows to state that the strain-rate sensitivity of the syntactic foam is mainly determined by the matrix.

As mentioned before, the parameter m is useful to obtain a good approximation in the elastic region of the stress–strain curve, without any influence in the plateau region or in the densification part [16]. This parameter is therefore strongly dependent on the type of test, since it contains also the information about the stiffness of the entire testing machine. Moreover, in high strain-rate tests, this parameters loses further of importance since the Hopkinson bar test is quite inaccurate and unreliable in the elastic region. From all these considerations, in the Table 3 only the average values obtained from the static experimental data were reported for each weight percentage and for each type of glass.

The parameter B is strongly influenced by several factor, such as the maximum level of strain reached, the initial specimen length and the type of experimental test performed. In general, the model is able to perform a good interpolation of the

Table 3
Final set of the analytical model parameters for the two foams varying the glass content.

Parameter (Unit)	S60HS			iM30K		
	5 (wt%)	10 (wt%)	13 (wt%)	5 (wt%)	10 (wt%)	13 (wt%)
A_0 (MPa)	252	234	182	270	264	245
A_1 (–)	0.0843	0.0871	0.0955	0.0901	0.0832	0.0688
$\dot{\varepsilon}_0$(1/s)	1.603	4.77	2.66	2.21	5.20	2.04
m (–)	32.9	49.8	118	32.6	61.5	60.7
B_0 (MPa)	1396	2874	–	1029	2050	142
n (–)	2.46	3.472	–	2.10	2.88	1.56
p (–)	0.532	0	–	0.707	0	1.47

each experimental curve, as shown in Fig. 9. The problem is that the results obtained from the interpolations present a great dispersion, especially in the dynamic regime. Nevertheless, looking the experimental stress–strain curves, it is possible to assert that passing from quasi-static to dynamic regime, the shape of the curves after the plateau is quite unchanged and the curves remain more or less parallel to each other (except for the 13 wt% curves, in which the material becomes probably too brittle and the fail-ure of the specimens avoid the increase of the stress value). This aspect is reflected in considering the parameter B substantially as strain-rate independent. The dispersion in the B values obtained as results of the model fit on each curve does not allow to extrapolate a global trend of this parameter varying the strain-rate (confirming the experimental data observation) or the wt% of glass. Based on this considerations, the model of Eq. (1) could be simplified considering $B_1 = 0$, while the parameter B_0 reported in Table 3 is the static average value.

In Fig. 12 the engineering stress–strain curves are compared with the results obtained with the model parameters of Table 3. For each microsphere content and for each strain-rate, only a curve is shown for sake of clarity both in case of S60HS and iM30K syntactic foams. As it is clear, in general, the model is able to predict with a good accuracy the materials behavior, espe-cially in quasi-static and medium strain-rate regimes. At high loading rate and over a certain level of strain, probably, some iner-tial phenomena occur, such that the material response is higher respect to the expected one. In quasi-static regime, the failures occurring in the material should have a sufficient time to propagate, decreasing the global strength of the foam. On the contrary, when the material is loading at high dynamic rate, the inertia or the friction between the damaged fragments could involve an increase in the material strength due to a greater difficulty of moldering.

6. Conclusions

The mechanical behavior of syntactic foams made of glass microspheres mixed in an iron matrix was investigated. This type of material is interesting since when compared to other types of metal foams it combines lower maximum porosity and higher density with greatly increased quasi-static compressive strength. Moreover it maintains the advantages and useful properties of metal foams such as thermal and environmental resistance. The syntactic foam analyzed in this work have an iron matrix with the dispersion of glass micro bubbles. Different types of foams were investigated varying the strength of the glass and its weight percentage content.

In particular the strain-rate sensitivity response was studied. To the authors' knowledge, this type of information was not studied previously for this material variant. The experimental characterization was performed by means of compression tests at three strain-rate levels, with three different experimental devices. At the highest strain-rate level a SHPB was used. The influence of type of glass spheres and their content was also studied.

The experimental results showed the compression behavior of syntactic foams, although generally similar to other types of foams, is strongly affected by all the examined factors. A little percentage of glass implies a pronounced drop in the material strength respect to the pure material. A further increase in the glass reduces the drop, probably since the contribution of glass microspheres balances the effect of the reduction of the metallic phase content. The results in case of the glass with a lower strength (S60HS) shows a more brittle and weaker behavior of the foam respect to the other (iM30K), which appears to have a more ductile behavior. For what concerns the strain-rate, it increases the material characteristics in almost all the responses. Both of the materials showed approximately the same response increasing the loading rate, and in this sense, the foams behavior is very similar to that of the metal matrix.

In order to evaluate the results obtained with the described tests campaign, the experimental data were further analyzed by means of an empirical analytical model. The model used is composed by two parts: a term describes the elastic and plastic behavior until the plateau; the other term describes the densification region. The dependency of the material response on the model parameters was widely discussed. In particular the material model was useful to clearly identify some typical parameters which evaluate the foam behavior, like the yield or plateau stress and to evaluate the influence of both strain-rate and glass content on these factors. The analysis was performed interpolating each experimental curve with the model and then evaluating the trend of the optimized parameters. The influence of the strain-rate on the plateau stress level was described using a Johnson-Cook formulation. The results showed the strain-rate behavior of the foams is mainly governed by the matrix. The other model parameters were not considered as strain-rate sensitive. This was justified by the fact that, from the experimental results, it was observed that (after the plateau) in the densification region the curves seem to remain parallel to each other. Moreover, the maximum strain levels reached in the experimental campaign did not ensure unique and reliable results for the model fit in the densification region. The model parameter correlated to the definition of slope of the elastic region was considered of little importance since it is useful to obtain a good fit in this region without any consequence on the remaining part of the model. In case of high percentage of glass for the S60HS-based foam, the model was not able to reproduce the after plateau region due to the fact that the experimental curves showed a slightly decreasing slope in the plateau without the presence of the densification. The last step was to obtain a single set of model parameters for each type and percentage of glass. The analytical data were compared with the experimental ones, and the results showed the model is able to reproduce with a satisfactory level of accuracy the material behavior, both in static and dynamic regime as well as for both the two types of glass and their percentage content.

References

[1] D.K. Balch, J.G. O'Dwyer, G.R. Davis, C.M. Cady, G.T. Gray III, D.C. Dunand, Mater. Sci. Eng. A 391 (2005) 408–417.
[2] X.F. Tao, Y.Y. Zhao, Scripta Mater. 61 (2009) 461–464.
[3] C. Swetha, R. Kumar, Mater. Design 32 (2011) 4152–4163.
[4] N. Gupta, V.C. Shunmugasamy, Mater. Sci. Eng. A 528 (2011) 7596–7605.
[5] V.C. Shunmugasamy, N. Gupta, Q. Nguyen, P.G. Coelho, Mater. Sci. Eng. A 527 (2010) 6166–6177.
[6] N. Gupta, R. Ye, M. Porfiri, Compos. B 41 (2010) 236–245.
[7] P.H. Viot, K. Shankar, D. Bernard, Compos. Struct. 86 (2008) 314–327.
[8] P.K. Rohatgi, N. Gupta, B.F. Schultz, D.D. Luong, JOM – J. Min. Met. Mater. Soc. 63 (2011) 36–42.
[9] Z.Y. Dou, et al., Scripta Mater. 57 (2007) 945–948.
[10] D.P. Mondal, et al., Mater. Design 34 (2012) 82–89.
[11] P. Viot, A. Chirazi, M. Dumon, D. Bernard, V. Fascio, Adv. Mater. Res. 146–147 (2010) 42–62.
[12] J. Lim, B. Smith, D.L. McDowell, Acta Mater. 50 (11) (2002) 2867–2879.
[13] D. Lehmhus, J. Baumeister, L. Stutz, E. Schneider, K. Stöbener, M. Avalle, L. Peroni, M. Peroni, Adv. Eng. Mater. 12 (2010) 596–603.
[14] M. Vesenjak, T. Fiedler, Z. Ren, A. Öchsner, Adv. Eng. Mater. 10 (12) (2008) 185–191.
[15] J. Weise, N. Salk, O. Yezerska, M. Schmitt, in: G. Stephani, B. Kieback (Eds.), Proc. Inter. Symp. Cellular Metals for Structural and Functional Applications, Fraunhofer IRB Verlag, Stuttgart, 2009, pp. 353–358.
[16] L. Peroni, M. Avalle, M. Peroni, Int. J. Mater. Eng. Innov. 1 (2009) 154–174.
[17] B.P. Neville, A. Rabiei, Mater. Design 29 (2008) 388–396.
[18] J. Weise, V. Zanetti-Bueckmann, O. Yezerska, M. Schneider, M. Haesche, Adv. Eng. Mater. 9 (2007) 52–56.
[19] L. Peroni, M. Avalle, M. Peroni, Int. J. Impact Eng. 35 (2008) 644–658.
[20] J.R. Johnson, W.H. Cook, 7th Int. Symposium on Ballistic, 1983, pp. 541–547.
[21] K.C. Rusch, J. Appl. Polym. Sci. 14 (1970) 1433–1447.
[22] B. Gladman, et al., LS-DYNA® Keyword User's Manual, vol. I, Version 971, LSTC, 2007.